

Optical Absorption Spectra and Dynamic Jahn-Teller Effect of V^{2+} Ions in ZnSe

Yi-Yang Zhou

Institute of Solid State Physics, Sichuan Normal University, Chengdu 610066, Sichuan, P. R. China

Reprint requests to Y.-Y. Z.; yiyazhou@mail.sc.cninfo.net

Z. Naturforsch. **63a**, 830–838 (2008); received May 5, 2008

The Hamiltonian matrices for $3d^3$ ions in a cubic crystal field are introduced, based on a molecular orbital model, including the electronic Coulomb and tetrahedral crystal-field interactions and the spin-orbit coupling. The optical absorption spectra of V^{2+} ions in ZnSe are studied. Moreover, the various additional levels found close to 5680 cm^{-1} are considered. These levels are assumed to result from the dynamic Jahn-Teller splitting within the excitation levels 2T_2 and 2T_1 in ZnSe: V^{2+} . The good agreement between the present results and the experimental observations indicates that the contribution of the covalence reduction factors N_E and N_{T_2} and of the Racah parameter A to the optical absorption spectra of V^{2+} ions in ZnSe is important. However, most of the previous theoretical studies of these spectra in ZnSe: V^{2+} have neglected the Racah parameter A , based on the classical crystal-field model. A significant charge-transfer effect found in recent works is confirmed in ZnSe: V^{2+} .

Key words: Semimagnetic Semiconductors; Optical Absorption Spectra; Dynamic Jahn-Teller Effect; V^{2+} Ions; ZnSe.

1. Introduction

Semimagnetic semiconductors (SMSCs) or diluted magnetic semiconductors (DMSCs) are II-V, II-VI, III-V and IV-VI compounds, where some nonmagnetic cations are substituted by magnetic ions of transition metals or rare-earth metals [1–3]. These systems exhibit interesting magnetic and magneto-optical properties due to the exchange interaction between the magnetic ions (d-d exchange) as well as between the magnetic ions and the bound electrons (s, p-d exchange) (see, e. g., [4–12]). The optical and magnetic properties of V^{2+} ions in the II-VI semiconductor ZnSe have been extensively studied in the past few decades (see, e. g., [13–20]). Because of the interesting infrared luminescence due to the internal transition within V^{2+} , attention has recently been paid to the important infrared window material ZnSe: V^{2+} [21, 22]. However, most of the theoretical studies on SMSCs were based on a simple crystal-field (CF) model. The CF model [23, 24] deals with the central transition-metal or rare-earth-metal ions as a quantum system with the corresponding wave function φ_d (d the outmost electrons of the ion), and treats the ligands as classical ones which provide only an electrostatic potential field V for the central metal ion. This means that the electrons of

the ligands are not allowed to overlap and mix with the electrons of the central metal ion. ZnSe has the zincblende structure [25, 26], the local symmetry is tetrahedral (T_d). The Hamiltonian of a V^{2+} ion in ZnSe is taken as [23, 24]

$$H = H_e + H_{CF} + H_{SO}, \quad (1)$$

where $H_e = H(A, B, C)$ and $H_{SO} = H(\zeta_d)$ are the electronic Coulomb interaction and the spin-orbit (SO) coupling of central metal ions, respectively, A , B , and C are the Racah parameters, ζ_d is the SO parameter. $H_{CF} = V = H(Dq)$ is the CF potential caused by the ligands, Dq the cubic CF parameter. Note that for V^{2+} ($3d^3$) ions the same values of the Racah parameters $3A$ appear in all diagonal matrices of the Hamiltonian (1). Therefore they are ignored in the calculation.

The simple CF model has difficulties to explain the absorption spectra of the V^{2+} ions in ZnSe. The simplest calculation of these spectra of ZnSe: V^{2+} is based on the ionic crystal approximation, in which the Racah parameters are $B = B_0 = 766\text{ cm}^{-1}$ and $C = C_0 = 2855\text{ cm}^{-1}$ [23] for the V^{2+} ion, and the measured $10Dq = 5000\text{ cm}^{-1}$ [13, 15] for ZnSe: V^{2+} is adopted. The subscript 0 corresponds to the free-ion system, similarly hereafter. The calculated results are listed in

Table 1. Comparison between the calculated and the experimental absorption spectra in ZnSe:V²⁺ (in cm⁻¹).

Experiment [15]	T	Calculations					
		This work	SO	α	β	γ	γ'
	⁴ T ₁	0	(^{0,77} _{306,465})	0	0	0	0
	² E	1941	(2192)				3027
3360	⁴ T ₂	3661	(^{3791,3809} _{3930,3963})	4271	4023	3358	3293
5685	² T ₂	5713	(⁵⁸⁴³ ₆₀₁₁)	8886	5739	4532	6107
6305	² T ₁	6031	(⁶²⁵¹ ₆₃₃₄)	9271	8623	7239	6215
8225	² T ₂	7778	(⁷⁹³² ₇₉₃₉)	12668	9298	7617	6505
8405	⁴ A ₂	7901	(8137)	12738	9548	7723	8027
8765	⁴ T ₁	8799	(^{8894,9027} _{9119,9135})	15032	10225	9759	8136
8905	² T ₂	9190	(¹⁰⁰⁵² ₁₀₀₅₈)	15900	11687	9948	8654
	² A ₁	9811	(10130)	16338	12746	10364	9570
	² T ₁	11153	(¹¹²⁶⁹ ₁₁₄₆₂)	18295	13938	11605	10077
12650	² E	12058	(12269)	18891	14477	12143	10802
13160	² T ₂	13178	(¹³³⁹⁵ ₁₃₄₅₆)	20274	15552	13030	12018
13850	² T ₁	13748	(¹³⁸⁵² ₁₄₁₂₈)	22301	17027	14448	12512
14470	² E	14810	(15102)	22729	17603	14954	12831
	² T ₂	15285	(¹⁵³⁸¹ ₁₅₆₂₉)	22782	18460	15198	14960
	² A ₂	17250	(17501)	29841	20419	18411	16038
	² T ₁	17615	(¹⁷⁷⁹⁸ ₁₈₀₃₆)	30684	21786	19427	16065
	² E	25388	(25509)	31220	21883	19593	23448
	² T ₂	25540	(²⁵⁸²⁶ ₂₅₉₉₈)	46407	32575	28768	23676
				46420	33180	28934	

α) $B = 766 \text{ cm}^{-1}$, $C = 2855 \text{ cm}^{-1}$, and $Dq = 500 \text{ cm}^{-1}$; β) $B = 452 \text{ cm}^{-1}$, $C = 2305 \text{ cm}^{-1}$, and $Dq = 460 \text{ cm}^{-1}$; γ) $B_0 = 766 \text{ cm}^{-1}$, $C_0 = 2855 \text{ cm}^{-1}$, and $Dq_0 = 500 \text{ cm}^{-1}$, $N = 0.881$; γ') $B_0 = 766 \text{ cm}^{-1}$, $C_0 = 2855 \text{ cm}^{-1}$, and $Dq_0 = 500 \text{ cm}^{-1}$, $N = 0.834$; T) $A = 11873 \text{ cm}^{-1}$, $B = 766 \text{ cm}^{-1}$, $C = 2855 \text{ cm}^{-1}$, and $Dq = 500 \text{ cm}^{-1}$, $N_E = 0.815$, $N_{T_2} = 0.855$ ($\zeta_d = 167$ and $\zeta_p = 1659 \text{ cm}^{-1}$).

set α of Table 1. Obviously the calculated energy levels are much larger than the observed ones. It shows clearly that the ionic crystal approximation is not suitable for the covalent crystals, especially for semiconductors. An earlier simple approximation method was trying to fit the experiments by artificially reducing the parameters B , C , and Dq . For example, one took $B = kB_0$ ($k < 1$) and $C = k'C_0$ ($k' < 1$) (see, e. g., [27–30]) or $B = kB_0$ ($k < 1$) and $C = k'B$ ($k' \gg 1$) (see, e. g., [13–15, 31]). When the reduced values [15] of $B = 452 \text{ cm}^{-1}$, $C = 2305 \text{ cm}^{-1}$, and $Dq = 460 \text{ cm}^{-1}$ for V²⁺:ZnSe are used, the corresponding calculated values, especially for the second and third excitation levels, indicate remarkable differences with the measured data. The calculated results are shown in set β of Table 1. In the late 1980s, a parametrized covalent approximation was proposed [32] as

$$B = N^4 B_0, \quad C = N^4 C_0, \quad Dq = N^2 Dq_0, \quad (2)$$

where $N < 1$ is the so-called covalence reduction factor. This model reduces the approximation procedure from adjusting three parameters, B , C , and Dq , to only

one covalence reduction factor N . It has been applied in many covalent materials (see, e. g., [33–36]). Taking $B_0 = 766 \text{ cm}^{-1}$, $C_0 = 2855 \text{ cm}^{-1}$ [23], and $Dq_0 = 500 \text{ cm}^{-1}$ [13, 15], the best fitted values compared with the observed data are listed in set γ of Table 1, where $N = 0.882$ is used. The results are similar to those shown in set β of Table 1. However, there are still differences between the calculated and the measured values.

2. Theoretical Model

Recent theoretical studies based on a molecular orbital (MO) model revealed the importance of ligand contribution to the optical and magnetic properties of Fe²⁺ [37–40] and Cr²⁺ [41–44] ions in II–VI semiconductors. The orbitals of the MO model are linear combinations of the d orbitals of V²⁺ and the outermost s and p orbitals of Se in ZnSe as given by [39, 42, 45–47]

$$\psi_i = N_E \left(\varphi_{di} - \sqrt{3} \lambda_{p\pi} \chi_{pi} \right),$$

$$\psi_j = N_{T_2}(\varphi_{dj} - \lambda_s \chi_{sj} - \lambda_{p\pi} \chi_{p\pi j} - \lambda_{p\sigma} \chi_{p\sigma j}) \quad (3)$$

with the normalization constants

$$\begin{aligned} N_E &= (1 + 3\lambda_{p\pi}^2 - 2\lambda_{p\pi} S_{p\pi})^{-1/2}, \\ N_{T_2} &= (1 + \lambda_s^2 + \lambda_{p\pi}^2 + \lambda_{p\sigma}^2 - 2\lambda_s S_s \\ &\quad - 2\lambda_{p\pi} S_{p\pi} - 2\lambda_{p\sigma} S_{p\sigma})^{-1/2}, \end{aligned} \quad (4)$$

where i and j stand for the cubic field representation [23, 24] $E(\theta, \varepsilon)$ and $T_2(\xi, \eta, \zeta)$, respectively. The wave functions φ_{di} and φ_{dj} represent the d orbitals of the central transition-metal ion (V^{2+}), whereas $\chi_{p\pi i}$, χ_{sj} , $\chi_{p\pi j}$ and $\chi_{p\sigma j}$ [45, 48, 49] are the appropriate symmetry-adopted combinations of the outermost s , p_π , and p_σ orbitals of the ligands (Se). λ_s , $\lambda_{p\pi}$, and $\lambda_{p\sigma}$ are the admixture coefficients, and S_s , $S_{p\pi}$, and $S_{p\sigma}$ are the two-center overlap integrals between the central ion and the ligands defined as

$$\begin{aligned} S_s &= \langle \varphi_{d\xi} | \chi_{s\xi} \rangle, \quad S_{p\pi} = \langle \varphi_{d\xi} | \chi_{p\pi\xi} \rangle, \\ S_{p\sigma} &= \langle \varphi_{d\xi} | \chi_{p\sigma\xi} \rangle. \end{aligned} \quad (5)$$

Equations (3)–(5) clearly explain the characteristics of the MO model. Compared with those in the CF model [23, 24], the ligands in the MO model are not treated as classical system anymore, and their orbitals are mixed and overlapping with the central metal ion orbitals.

The normalization constants N_E and N_{T_2} in (3) and (4) are just the covalence reduction factors. For the difference of N_E and N_{T_2} , the Hamiltonian matrices of H_e and H_{CF} in (1) are as follows:

$${}^4A_2[t^3]: 3A_1 - 15B_1 - 12Dq_1; \quad (6a)$$

$${}^4T_2[t^2({}^3T_1)e]: A_1 - 5B_1 + 2A_3 \\ - 10B_3 - 8Dq_1 + 6Dq_2; \quad (6b)$$

$${}^2A_1[t^2({}^1E)e]: A_1 + B_1 + 2C_1 + 2A_3 - 12B_3 \\ + C_3 - 8Dq_1 + 6Dq_2; \quad (6c)$$

$${}^2A_2[t^2({}^1E)e]: A_1 + B_1 + 2C_1 + 2A_3 + 8B_3 \\ + C_3 - 8Dq_1 + 6Dq_2; \quad (6d)$$

$$\begin{aligned} {}^4T_1[t^2({}^3T_2)e]: & {}^4T_{11} \quad -6B_4 \\ {}^4T_1[te^2({}^3A_2)]: & {}^4T_{12}, \end{aligned} \quad (6e)$$

with

$$\begin{aligned} {}^4T_{11} &= A_1 - 5B_1 + 2A_3 + 2B_3 - 8Dq_1 + 6Dq_2, \\ {}^4T_{12} &= A_2 - 8B_2 + 2A_3 - 4B_3 - 4Dq_1 + 12Dq_2; \end{aligned} \quad (6e')$$

$$\begin{aligned} {}^2E[t^3]: & {}^2E_1 - 6\sqrt{2}B_4 - 3\sqrt{2}B_4 \quad 0 \\ {}^2E[t^2({}^1A_1)e]: & {}^2E_2 \quad 10B_3 \quad \sqrt{3}(2B_3 + C_3) \\ {}^2E[t^2({}^1E)e]: & {}^2E_3 \quad 2\sqrt{3}B_3 \\ {}^2E[e^3]: & {}^2E_4, \end{aligned} \quad (6f)$$

with

$$\begin{aligned} {}^2E_1 &= 3A_1 - 6B_1 + 3C_1 - 12Dq_1, \\ {}^2E_2 &= A_1 + 10B_1 + 5C_1 + 2A_3 - 2B_3 \\ &\quad + C_3 - 8Dq_1 + 6Dq_2, \\ {}^2E_3 &= A_1 + B_1 + 2C_1 + 2A_3 - 2B_3 \\ &\quad + C_3 - 8Dq_1 + 6Dq_2, \\ {}^2E_4 &= 3A_2 - 8B_2 + 4C_2 + 18Dq_2; \end{aligned} \quad (6f')$$

$$\begin{aligned} {}^2T_1[t^3]: & {}^2T_{11} \quad 3B_4 - 3B_4 \quad 0 \quad -2\sqrt{3}B_3 \\ {}^2T_1[t^2({}^3T_1)e]: & {}^2T_{12} - 3B_3 \quad 3B_4 \quad -3\sqrt{3}B_4 \\ {}^2T_1[t^2({}^1T_2)e]: & {}^2T_{13} - 3B_4 \quad \sqrt{3}B_4 \\ {}^2T_1[te^2({}^1A_2)]: & {}^2T_{14} \quad -2\sqrt{3}B_3 \\ {}^2T_1[te^2({}^1E)]: & {}^2T_{15}, \end{aligned} \quad (6g)$$

with

$$\begin{aligned} {}^2T_{11} &= 3A_1 - 6B_1 + 3C_1 - 12Dq_1, \\ {}^2T_{12} &= A_1 - 5B_1 + 2A_3 + 5B_3 + 3C_3 \\ &\quad - 8Dq_1 + 6Dq_2, \\ {}^2T_{13} &= A_1 + B_1 + 2C_1 + 2A_3 - 7B_3 + C_3 \\ &\quad - 8Dq_1 + 6Dq_2, \\ {}^2T_{14} &= A_2 - 8B_2 + 2A_3 + 2B_3 + 3C_3 \\ &\quad - 4Dq_1 + 12Dq_2, \\ {}^2T_{15} &= A_2 + 2C_2 + 2A_3 - 2B_3 + C_3 \\ &\quad - 4Dq_1 + 12Dq_2; \end{aligned} \quad (6g')$$

$$\begin{aligned} {}^2T_2[t^3]: & {}^2T_{21} \quad -3\sqrt{3}B_4 \quad -5\sqrt{3}B_4 \quad 4B_3 + 2C_3 \quad -2B_3 \\ {}^2T_2[t^2({}^3T_1)e]: & {}^2T_{22} \quad 3B_3 \quad -3\sqrt{3}B_4 \quad 3\sqrt{3}B_4 \\ {}^2T_2[t^2({}^1T_2)e]: & {}^2T_{23} \quad -\sqrt{3}B_4 \quad \sqrt{3}B_4 \\ {}^2T_2[te^2({}^1A_1)]: & {}^2T_{24} \quad -10B_3 \\ {}^2T_2[te^2({}^1E)]: & {}^2T_{25}, \end{aligned} \quad (6h)$$

with

$$\begin{aligned}
 {}^2T_{21} &= 3A_1 + 5C_1 - 12Dq_1, \\
 {}^2T_{22} &= A_1 - 5B_1 + 2A_3 - B_3 \\
 &\quad + 3C_3 - 8Dq_1 + 6Dq_2, \\
 {}^2T_{23} &= A_1 + B_1 + 2C_1 + 2A_3 + 3B_3 \\
 &\quad + C_3 - 8Dq_1 + 6Dq_2, \\
 {}^2T_{24} &= A_2 + 8B_2 + 4C_2 + 2A_3 - 2B_3 \\
 &\quad + C - 4Dq_1 + 12Dq_2, \\
 {}^2T_{25} &= A_2 + 2C_2 + 2A_3 - 2B_3 + C_3 \\
 &\quad - 4Dq_1 + 12Dq_2.
 \end{aligned} \tag{6h'}$$

The matrix is real and symmetric, and only the blocks on and above the diagonal are shown in (6e), (6f), (6g), and (6h). The 10 Racah and 2 cubic CF parameters presented are [39, 42]

$$\begin{aligned}
 (A_1, B_1, C_1) &= N_{T_2}^4(A, B, C), \\
 (A_2, B_2, C_2) &= N_E^4(A, B, C), \\
 (A_3, B_3, C_3) &= N_{T_2}^2 N_E^2(A, B, C), \\
 B_4 &= N_{T_2}^3 N_E B;
 \end{aligned} \tag{7}$$

$$Dq_1 = N_{T_2}^2 Dq, \quad Dq_2 = N_E^2 Dq. \tag{8}$$

Please note that the Racah parameters A_i ($i = 1-3$) in the diagonal matrices are not identical. Therefore, they cannot be neglected in this model.

For the difference of N_E and N_{T_2} , the complex matrices of H_{SO} in (1) are also obtained. There are two SO parameters [39, 42],

$$\begin{aligned}
 \zeta_1 &= N_{T_2}^2 \left[\zeta_d + \left(\sqrt{2} \lambda_{p\sigma} \lambda_{p\pi} - \lambda_{p\pi}^2 / 2 \right. \right. \\
 &\quad \left. \left. - \sqrt{2} \lambda_s \lambda_{p\pi} S_{sp} \right) \zeta_p \right], \\
 \zeta_2 &= N_E N_{T_2} \left[\zeta_d + \left(\lambda_{p\sigma} \lambda_{p\pi} / \sqrt{2} + \lambda_{p\pi}^2 / 2 \right. \right. \\
 &\quad \left. \left. - \lambda_s \lambda_{p\pi} S_{sp} / \sqrt{2} \right) \zeta_p \right],
 \end{aligned} \tag{9}$$

with the overlap integral

$$S_{sp} = R \langle \chi_{p_y} | \partial / \partial y | \chi_s \rangle, \tag{10}$$

where R is the distance between the central ion and the ligands, ζ_d and ζ_p are the SO coupling constants associated with the d electrons of the central metal ion (V²⁺) and p electrons of the ligands (Se), respectively.

The details of the derivation of the SO coupling matrices can be found in [50, 51]. From (9), one may notice that the SO coupling not only within the V²⁺ ions but also within the ligands Se is considered in this model.

It should be pointed out that the present model may be reduced to the parametrized covalent approximation [32] by taking $\lambda_s = \lambda_{p\pi} = \lambda_{p\sigma} = S_s = S_{p\pi} = S_{p\sigma} = 0$ and $N_{T_2} = N_E < 1$, and to the CF approximation [23, 24] by taking $\lambda_s = \lambda_{p\pi} = \lambda_{p\sigma} = S_s = S_{p\pi} = S_{p\sigma} = 0$ and $N_{T_2} = N_E = 1$ (i. e., there are no admixtures and overlaps between the central ion and the ligands, and the d orbitals φ_d of the central metal ion are the only wave functions considered).

3. Optical Absorption Spectra

In this work, the values of $A = A_0 = 11873 \text{ cm}^{-1}$ [52], $B = B_0 = 766 \text{ cm}^{-1}$, and $C = C_0 = 2855 \text{ cm}^{-1}$ [23, 52] for the V²⁺ ion, and $Dq = 500 \text{ cm}^{-1}$ [14, 15] for V²⁺:ZnSe are adopted. Using (7) and (8), the absorption spectra can be calculated by adjusting the covalence reduction factors N_E and N_{T_2} . From the definition of N_E and N_{T_2} by (4), the values of the admixture coefficients λ_s , $\lambda_{p\pi}$, and $\lambda_{p\sigma}$ and the overlap integrals S_s , $S_{p\pi}$, and $S_{p\sigma}$ should be given first. When the value [25] of $R(\text{Zn-Se}) = 0.245 \text{ nm}$ in ZnSe is used for V-substituted ZnSe, the values of the overlap integrals $S_s = 0.03959$, $S_{p\pi} = 0.02305$, $S_{p\sigma} = 0.07754$, and $S_{sp} = 1.93963$ can be obtained from a Slater-type orbital [53, 54]. The values of the admixture coefficients λ_s , $\lambda_{p\pi}$ and $\lambda_{p\sigma}$ remain unknown, and the present work adopts the procedure [40, 42, 55] of fitting the experimental optical spectra using λ_s , $\lambda_{p\pi}$ and $\lambda_{p\sigma}$. The set of admixture coefficients that explains the experimental data best is $\lambda_s = 0.115$, $\lambda_{p\pi} = 0.418$, and $\lambda_{p\sigma} = 0.429$. Above values of S_i and λ_i yield the covalence reduction factors $N_E = 0.815$ and $N_{T_2} = 0.855$. The corresponding calculated results of the optical spectra as shown in set T of Table 1 are in good agreement with the experimental ones. It should be pointed out that, when compared with the sets α , β , and γ , the set T seems to move downwards, as a whole. Also a near-infrared level, 1941 cm^{-1} , is calculated, which has not been reported in the previous experimental results. Further theoretical and experimental check of this level is necessary.

Following the present procedure, the set γ (obtained from the parameterized covalent approximation [32]) may also be moved by adjusting N . The correspond-

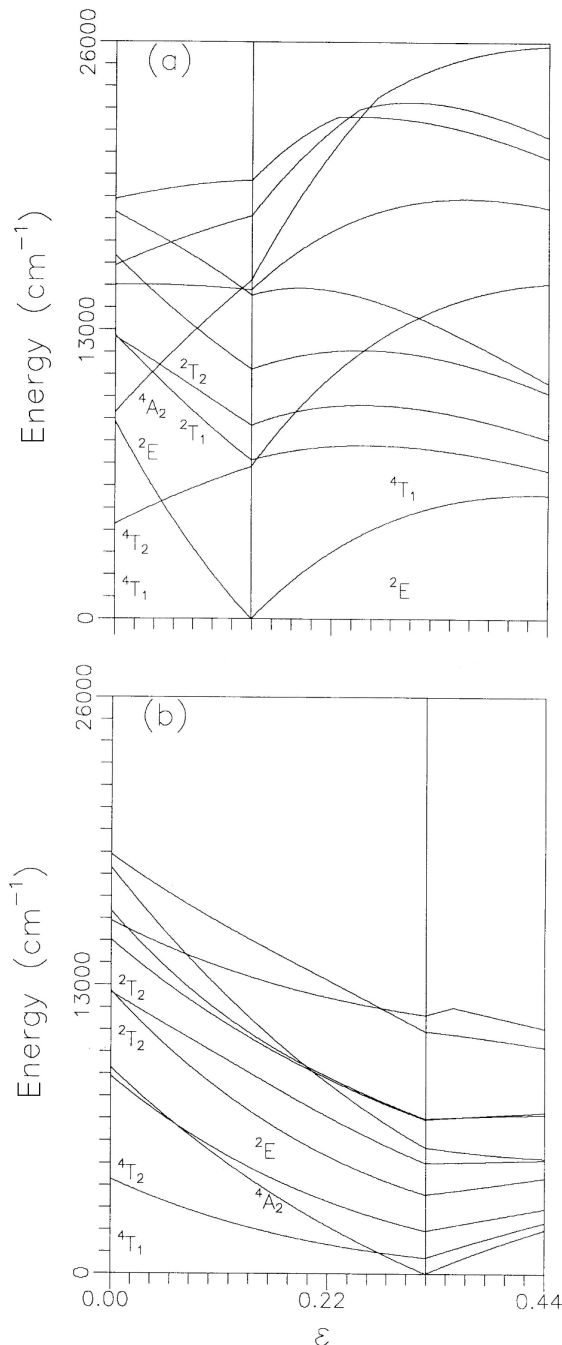


Fig. 1. The variation of the energy levels with the covalence parameter $\varepsilon = 1 - N_E$ ($N_{T_2} = 1$). (a) $A = 11873$, $B = 766$, $C = 2855$, and $Dq = 500$ (all in cm^{-1}). (b) $A = 0$, $B = 766$, $C = 2855$, and $Dq = 500$ (all in cm^{-1}).

ing calculated data with $N = 0.834$ are shown in the set γ' of Table 1. The values in set γ' are moved down-

wards as compared with those in set γ . However, there remains a considerable difference between the calculated numbers in set γ' and the experiments. It seems likely that the difference between the present model and the parameterized covalent approximation is just a matter of how many factors to adjust, i. e., two covalence reduction factors N_E and N_{T_2} or one factor N . However, the true, essential distinction lies in the MO and CF model, as mentioned above. Particularly, the MO model considers the contribution of the Racah parameter A whose size is much larger than those of B and C .

To show the contribution of the Racah parameter A at different angle, the variations of the first 10 energy levels via the covalence parameters $\varepsilon = 1 - N_E$ and $\varepsilon = 1 - N_{T_2}$ are plotted in Figs. 1 and 2, respectively, where subfigures (a) and (b) correspond to $A = 11873 \text{ cm}^{-1}$ and $A = 0$, respectively. Obviously, the larger the size of ε , the smaller is the value of the covalence reduction factors N_E or N_{T_2} , i. e., the stronger is the covalence. In both Figures, together with some small changes of ε there is a significant change of the energy levels. This phenomenon indicates the important contribution of the covalence reduction factors N_E and N_{T_2} to the optical spectra of V^{2+} ions in ZnSe. One can see a large difference between Fig. 1a and 1b. For example, (i) on increasing $\varepsilon = 1 - N_E$ some excited levels increase while other levels decrease within $A \neq 0$, however for $A = 0$, all excited levels have the same pattern, first a decrease and then an increase; (ii) there is a change from the ground state 4T_1 to 2E for $A \neq 0$, however, the change of the ground state is from 4T_1 to 4A_2 for $A = 0$. Similarly, the same large difference between Figs. 2a and 2b exists, i. e. the ground state changes from 4T_1 to 4T_2 , then to 4A_2 , and finally to 4T_2 for $A \neq 0$; however, such change does not exist for $A = 0$. The difference between Figs. 1a and 1b as well as between Figs. 2a and 2b clearly shows the important contribution of the Racah parameter A to the energy levels.

It should be noted that the large values of the admixture coefficients λ_i in ZnSe:V^{2+} indicate that the contribution of the outermost s , p_σ , and p_π orbitals of the ligands Se to the molecular orbitals (3) is important. Such large values of λ_i have also been obtained in previous studies on Fe^{2+} [37–40] and Cr^{2+} [41–44] ions in the II-VI semiconductors ZnS, ZnSe, CdTe, etc. The introduction of the ligand orbitals causes the difference between the Racah parameters A_i , B_i , C_i and A , B , C and furthermore the important contribution of A . These

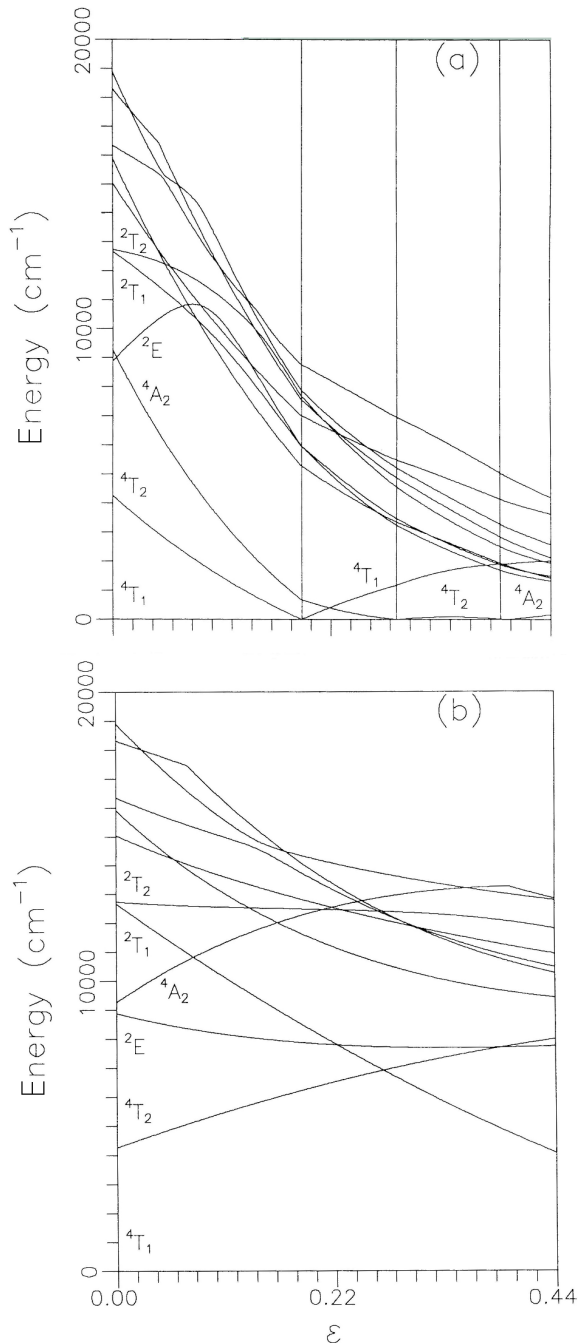


Fig. 2. The variation of the energy levels with the covalence parameter $\varepsilon = 1 - N_{T_2}$ ($N_E = 1$). (a) $A = 11873$, $B = 766$, $C = 2855$, and $Dq = 500$ (all in cm^{-1}). (b) $A = 0$, $B = 766$, $C = 2855$, and $Dq = 500$ (all in cm^{-1}).

values of λ_i can be used in first-order approximation to reduce the charge-transfer covalences by means of the

Table 2. Comparison between the observed and the calculated Jahn-Teller energies associated with the multiplets 2T_2 and 2T_1 in ZnSe:V²⁺ (in cm^{-1}).

Experiments [13, 15]	Calculation	($l+m+n=10$)
5675	Γ_4	5673
5685	Γ_4	5685
	Γ_3	5693
5705	Γ_4	5706
5715	Γ_4	5717
5724	Γ_3	5727
	Γ_5	5744
5765	Γ_4	5760
	Γ_4	5779
5790	Γ_5	5794
	Γ_3	5819
5840	Γ_5	5844
5862	Γ_4	5859
	Γ_5	5891
5915	Γ_4	5910

expressions [41, 45]

$$\lambda_i = S_i + \kappa_i \quad (i = s, p_\sigma, \text{ and } p_\pi), \quad (11)$$

where S_s , S_{p_σ} , and S_{p_π} have been defined by (5), and κ_i are the corresponding charge-transfer covalence parameters. The bonding orbitals can be modelled by combining the central ion d orbitals with the ligand orbitals by means of the charge-transfer covalence parameters κ_i . The calculated values of the charge-transfer covalences come out to be $\kappa_s = 0.075$, $\kappa_{p_\pi} = 0.395$, and $\kappa_{p_\sigma} = 0.351$. This clearly shows the significance of the charge-transfer effect in ZnSe:V²⁺.

4. Dynamic Jahn-Teller Effect Splittings

Wray and Allen [13] and Hoang and Baranowski [15] found some additional spectra structures (about 10 energy levels) from 5675 cm^{-1} to 5915 cm^{-1} as shown in Table 2. Wray and Allen assigned these levels as splitting of the 4A_2 state, while Hoang and Baranowski assumed that they are due to the splitting of the 2E state. However, according to the present work, these levels should be the splitting of 2T_2 as well as the nearby 2T_1 (see Table 1).

It is well known that the H_{SO} coupling in (1) might be able to move, but not to split the 4A_2 and 2E states. If taking the SO coupling parameters $\zeta_d = 167 \text{ cm}^{-1}$ [23, 56] for the V²⁺ ion and $\zeta_p = 1659 \text{ cm}^{-1}$ [56] for the ligands (Se) and then following the present calculation method, the fine splitting caused by the H_{SO} coupling is listed in the bracket of Table 1. One can see from Table 1 that the H_{SO} coupling moves the levels 1941 cm^{-1} (2E) and 7901 cm^{-1}

(⁴A₂) to 2192 cm⁻¹ and 8137 cm⁻¹, respectively, and splits the values of 5713 cm⁻¹ (²T₂) and 6031 cm⁻¹ (²T₁) into 5843 cm⁻¹ and 6011 cm⁻¹, and 6251 cm⁻¹ and 6334 cm⁻¹, respectively. Obviously, these changes caused by the SO coupling cannot explain the additional optical levels listed in Table 2. It means that to explain these levels, one has to consider another mechanism.

Bevilacqua, Martinelli, and Vogel [20] proposed a dynamic Jahn-Teller (JT) effect to interpret the fine structures of the luminescence spectra of V²⁺ impurities in ZnS and ZnSe. In their paper, the JT splitting of the electron orbital triplets ⁴T₁ and ⁴T₂ coupled with a τ phonon was considered [20]. In fact, the orbital triplet JT system $T \otimes \tau$ used to be cited in the literature (see, e. g., [57–61]) and the coupling of the orbital triplets ²T₂ and ²T₁ with the τ phonon were also mentioned [59]. The JT Hamiltonian is taken as [20, 60, 61]

$$H_{JT} = h\omega \sum_i (a_i^+ a_i + 1/2) + (h\omega E_{JT})^{1/2} \sum_i (a_i^+ + a_i) D_i, \quad (12)$$

$i = x, y, z,$

where $h\omega$ and E_{JT} are the phonon and JT energies, respectively, a_i (a_i^+) is the destruction (creation) operator for a phonon of the τ mode, and D_i are the normalized electronic operators as

$$D_x = \begin{pmatrix} 0 & 0 & 0 \\ 0 & 0 & 1 \\ 0 & 1 & 0 \end{pmatrix}, \quad D_y = \begin{pmatrix} 0 & 0 & 1 \\ 0 & 0 & 0 \\ 1 & 0 & 0 \end{pmatrix}, \quad (13)$$

$$D_z = \begin{pmatrix} 0 & 1 & 0 \\ 1 & 0 & 0 \\ 0 & 0 & 0 \end{pmatrix}.$$

The representation of the electron (²T₂: γ_5 and ²T₁: γ_4)-phonon (τ : γ_5^p) coupling is [62]

$$\begin{aligned} \gamma_5 \otimes \gamma_5^p &= \Gamma_1 \oplus \Gamma_3 \oplus \Gamma_4 \oplus \Gamma_5, \\ \gamma_4 \otimes \gamma_5^p &= \Gamma_2 \oplus \Gamma_3 \oplus \Gamma_4 \oplus \Gamma_5. \end{aligned} \quad (14)$$

The basic functions Γ_i ($i = 1-5$) in the vibronic model (14) are the direct product of the eigenfunctions of the Hamiltonian (1) and the vibrational functions $|mnl\rangle$ [63], where l , m , and n are the occupation numbers for the partners of the phonon τ mode. In principle, the occupation numbers run from zero to infinity. Using the above values of Racah, CF, and SO parameters, the dynamic JT splitting levels are calculated (see Table 2) by taking $h\omega = 67$ cm⁻¹, $E_{JT} = 113$ cm⁻¹

for ²T₁ and $E_{JT} = 223$ cm⁻¹ for ²T₂, which are near to the obtained values [20] of 70 cm⁻¹ and 110 cm⁻¹ for ²T₁ and 220 cm⁻¹ for ²T₂, respectively. The good agreement between the calculated and the measured fine levels indicates that the additional optical levels of the V²⁺ impurities in ZnSe are due to the JT splitting in the system. It further proves the validity of the above values for the Racah, CF, and SO parameters as well as the admixture coefficients (i. e., the covalence reduction factors). The good agreement between the calculated and the measured fine levels shows again that the present MO model is suitable for the V²⁺ impurities in ZnSe.

The present work reveals additional lines at 5693, 5744, 5779, 5819, and 5891 cm⁻¹. These lines were not reported in the existing experimental data material. There is a need for further experimental check for these lines.

5. Conclusion

A Hamiltonian matrix has been constructed for a 3d³ ion by a molecular orbital approach, including the electronic Coulomb and tetrahedral crystal-field interactions and the spin-orbit coupling. In the matrices there were 10 Racah, 2 cubic crystal-field, and 2 spin-orbit parameters. The matrix has been used to study the optical absorption spectra of V²⁺ impurities in the semiconductor ZnSe. The additional fine-structure levels were studied also. In the present calculation, the values of the Racah, crystal-field, and spin-orbit parameters were obtained by adjusting the admixture coefficients (i. e., the covalence reduction factors) that explain best the experimental data of the optical spectra and the additional fine levels. The contributions of the covalence reduction factors N_E and N_{T_2} , and of the Racah parameter A to the excitation levels were considered for the first time and found to be important in ZnSe:V²⁺. It was also the first time that the fine-structure levels from 5675 cm⁻¹ to 5915 cm⁻¹ were assumed to be the result of dynamic Jahn-Teller splitting within the excitation levels ²T₂ and ²T₁. A significant charge-transfer effect was found to be present in this system. Some theoretical near-infrared levels were not reported in the existing experimental data. There is need for further theoretical and experimental studies. The present model can be easily reduced to the crystal-field approximation, which is suitable for the study of transition-metal or rare-earth metal ions in ionic crystals.

Acknowledgements

This work was supported by the National Natural Science Foundation of China, the Scientific Founda-

tion of Education Department of Sichuan Province, China, as well as the Foundation of Sichuan Normal University.

- [1] J. K. Furdyna, *J. Appl. Phys.* **64**, R29 (1988); *Semiconductor and Semimetals in Diluted Magnetic Semiconductors*, Academic Press, New York 1988.
- [2] W. J. M. De Jonge and H. J. M. Swagten, in: *II-VI Semiconducting Compounds*, Plenum Press, New York 1991, p. 149.
- [3] J. Kossut and W. Dobrowolski, *Handbook of Magnetic Materials*, North-Holland, Amsterdam 1993.
- [4] H. J. M. Swagten, A. Twardowski, W. J. M. de Jonge, and M. Demianiuk, *Phys. Rev. B* **39**, 2568 (1989).
- [5] A. Twardowski, *J. Appl. Phys.* **67**, 5108 (1990).
- [6] W. J. M. de Jonge and H. J. M. Swagten, *J. Magn. Magn. Mater.* **111**, 322 (1991).
- [7] W. Mac, N. T. Khoi, A. Twardowski, and J. A. Gaj, *Phys. Rev. Lett.* **71**, 2327 (1993).
- [8] W. Mac, A. Twardowski, P. J. T. Eggenkamp, H. J. M. Swagten, Y. Sharira, and M. Demianiuk, *Phys. Rev. B* **50**, 14144 (1994).
- [9] W. Mac, A. Twardowski, and M. Demianiuk, *Phys. Rev. B* **54**, 5528 (1996).
- [10] D. Colignon, E. Kartheuser, and M. Villeret, *J. Phys.: Condens. Matter* **12**, 2691 (2000).
- [11] L. W. Yin and M. S. Li, *Adv. Materials* **12**, 1792 (2005).
- [12] C. F. Wang, Q. S. Li, L. Lu, L. Z. Zhang, H. X. Qi, and H. Chen, *Chin. Phys. Lett.* **24**, 825 (2007).
- [13] E. M. Wray and J. W. Allen, *J. Phys. C: Solid State Phys.* **4**, 512 (1968).
- [14] J. M. Langer and J. M. Baranowski, *Phys. Status Solidi (b)* **49**, 499 (1972).
- [15] L. M. Hoang and J. M. Baranowski, *Phys. Status Solidi (b)* **84**, 361 (1977).
- [16] S. Watanabe and H. Kamimura, *Mat. Sci. Eng. B* **3**, 313 (1989).
- [17] T. M. Wilsom, *Int. J. Quant. Chem.: Quant. Chem. Symp.* **24**, 187 (1990).
- [18] T. Mizokawa and A. Fujimori, *Phys. Rev. B* **48**, 14150 (1993).
- [19] O. Zakharov, A. Rubio, X. Blasé, M. L. Cohen, and G. Louie, *Phys. Rev. B* **50**, 10780 (1994).
- [20] G. Bevilacqua, L. Martinelli, and E. E. Vogel, *Phys. Rev. B* **66**, 155338 (2002).
- [21] L. G. Fu, C. S. He, and N. O. Lu, *Infrared Laser Eng.* **34**, 31 (2005).
- [22] Y. P. Yao and J. H. Liu, *J. Synth. Cryst.* **35**, 183 (2006).
- [23] J. S. Griffith, *The Theory of Transition Metal Ions*, Cambridge University Press, Cambridge 1960.
- [24] C. J. Ballhausen, *Introduction to Ligand Field Theory*, McGraw-Hill, New York 1962.
- [25] R. W. G. Wyckoff, *Crystal Structure*, Interscience, London 1987.
- [26] A. F. Wells, *Structural Inorganic Chemistry*, Oxford University Press, New York 1987.
- [27] C. K. Jorgensen, *Modern Aspects of Ligand Field Theory*, North-Holland, Amsterdam 1971.
- [28] C. A. Morrison, *Crystal Field for Transition-Metal Ions in Laser Host Materials*, Springer, Berlin 1992.
- [29] B. G. Burns, *Mineralogical Application of Crystal Field Theory*, Cambridge University Press, Cambridge 1993.
- [30] Z. Y. Yang, *J. Magn. Magn. Mater.* **238**, 200 (2002).
- [31] E. Kong and S. Kremer, *Z. Naturforsch.* **29a**, 31 (1974).
- [32] M. G. Zhao, M. L. Du, and G. Y. Shen, *J. Phys. C: Solid State Phys.* **20**, 5557 (1987).
- [33] M. L. Du and M. G. Zhao, *J. Phys. C: Solid State Phys.* **21**, 1561 (1988).
- [34] M. G. Zhao and M. Chiu, *Phys. Rev. B* **52**, 10053 (1995).
- [35] M. G. Zhao and Y. Lei, *Phys. Rev. B* **55**, 1 (1997).
- [36] W. C. Zheng, S. Y. Wu, and J. Zi, *Physica B* **315**, 223 (2002).
- [37] F. Z. Li and Y. Y. Zhou, *J. Phys. Chem. Solids* **58**, 1391 (1997).
- [38] F. Z. Li and Y. Y. Zhou, *Acta Phys. Sin.* **47**, 472 (1998).
- [39] Y. Y. Zhou, *Physica B* **322**, 61 (2002).
- [40] Y. Y. Zhou, *J. Appl. Phys.* **95**, 6870 (2004).
- [41] Y. Y. Zhou and F. Z. Li, *J. Phys.: Condens. Matter* **9**, 8631 (1997).
- [42] Y. Y. Zhou and F. Z. Li, *J. Phys. Chem. Solids* **59**, 1105 (1998).
- [43] D. H. Li, F. Z. Li, and Y. Y. Zhou, *Solid State Commun.* **105**, 59 (1998).
- [44] F. Z. Li, D. H. Li, and Y. Y. Zhou, *Physica B* **252**, 167 (1998).
- [45] S. Sugano, Y. Tanabe, and H. Kamimura, *Multiplets of Transition-Metal Ions in Crystals*, Academic Press, New York 1970.
- [46] Y. Y. Zhou and F. Z. Li, *Phys. Rev. B* **51**, 14175 (1995).
- [47] Y. Y. Zhou, *Phys. Status Solidi (b)* **243**, 4051 (2006).
- [48] C. J. Ballhausen, *Molecular Electronic Structures of Transition Metal Complexes*, McGraw-Hill, New York 1979.
- [49] A. S. Chakravarty, *Introduction to the Magnetic Properties of Solids*, John Wiley & Sons, New York 1980.
- [50] Y. Y. Zhou, *J. Sichuan Normal Univ. (Nat. Sci.)* **24**, 51 (2001) (in English).

- [51] Y. Y. Zhou, *J. Sichuan Normal Univ. (Nat. Sci.)* **24**, 157 (2001) (in English).
- [52] A. Many, *Phys. Rev.* **70**, 511 (1946).
- [53] E. Clementi and D. L. Raimondi, *J. Chem. Phys.* **38**, 2686 (1963).
- [54] E. Clementi, D. L. Raimondi, and W. P. Reinhardt, *J. Chem. Phys.* **47**, 1300 (1963).
- [55] M. H. de A. Viccra, S. Sundaram, and R. R. Sharma, *Phys. Rev. B* **25**, 773 (1982).
- [56] S. Fraga, K. M. S. Saxena, and J. Karwowski, *Handbook of Atomic Data*, Elsevier, New York 1976.
- [57] C. A. Bates and J. L. Dunn, *J. Phys.: Condens. Matter* **1**, 2605 (1989).
- [58] J. L. Dunn, *J. Phys.: Condens. Matter* **1**, 7861 (1989).
- [59] H. Kalkam, S. Atalay, and I. Senel, *Z. Naturforsch.* **53a**, 945 (1998).
- [60] L. Martinelli, G. Bevilacqua, J. Rivera-Ivera, M. A. de Orue, O. Mualin, E. E. Vogel, and J. Cartes, *Phys. Rev. B* **64**, 10873 (2000).
- [61] O. Mualin, E. E. Vogel, M. A. de Orue, L. Martinelli, G. Bevilacqua, and H. J. Schulz, *Phys. Rev. B* **65**, 035211 (2001).
- [62] G. F. Koster, J. O. Dimmock, R. G. Wheeler, and H. Statz, *Properties of the Thirty-Two Point Groups*, M.I.T., Cambridge 1963.
- [63] H. Maier and U. Scherz, *Phys. Status Solidi (b)* **62**, 153 (1974).